Induction of rod versus cone photoreceptor-specific progenitors from retinal precursor cells

Saeed Khalili[a,1], Brian G. Ballios[b,1], Justin Belair-Hickey[a], Laura Donaldson[c], Jeff Liu[a], Brenda L.K. Coles[a], Kenneth N. Grisé[a], Tahani Baakdhah[h], Gary D. Bader[a], Valerie A. Wallace[b,d], Gilbert Bernier[e,f], Molly S. Shoichet[g], Derek van der Kooy[a,*]

[a] Department of Molecular Genetics, University of Toronto, Toronto, Ontario M5S 1A8, Canada
[b] Department of Ophthalmology and Vision Sciences, University of Toronto, 340 College Street, Suite 400, Toronto, Ontario M5T 3A9, Canada
[c] Division of Ophthalmology, Department of Surgery, Faculty of Health Sciences, McMaster University, 2757 King Street East, Hamilton, Ontario L8G 4X3, Canada
[d] Donald K Johnson Eye Institute, Krembil Research Institute, University Health Network, 60 Leonard Ave., Rm 8KD413, Toronto, Ontario M5T 2S8, Canada
[e] Stem Cell and Developmental Biology Laboratory, Hôpital Maisonneuve-Rosemont, 5415 Boul. l'Assomption, Montréal H1T 2M4, Canada
[f] Faculté de Médecine, Département de Neurosciences, Université de Montréal, Montréal H3T 1J4, Canada
[g] Department of Chemical Engineering and Applied Chemistry, University of Toronto, 200 College Street, Toronto, Ontario M5S 3E5, Canada
[h] Institute of Medical Science, University of Toronto, 1 King's College Circle, Toronto, Ontario M5S 1A8, Canada

ARTICLE INFO

ABSTRACT

During development, multipotent progenitors undergo temporally-restricted differentiation into post-mitotic retinal cells; however, the mechanisms of progenitor division that occurs during retinogenesis remain controversial. Using clonal analyses (lineage tracing and single cell cultures), we identify rod versus cone lineage-specific progenitors derived from both adult retinal stem cells and embryonic neural retinal precursors. Taurine and retinoic acid are shown to act in an instructive and lineage-restricted manner early in the progenitor lineage hierarchy to produce rod-restricted progenitors from stem cell progeny. We also identify an instructive, but lineage-independent, mechanism for the specification of cone-restricted progenitors through the suppression of multiple differentiation signaling pathways. These data indicate that exogenous signals play critical roles in directing lineage decisions and resulting in fate-restricted rod or cone photoreceptor progenitors in culture. Additional factors may be involved in governing photoreceptor fates in vivo.

1. Introduction

Retinal cells are born in a prescribed and sequential manner during development (Turner and Cepko, 1987). Previous studies (Holt et al., 1988; Turner et al., 1990; Wetts and Fraser, 1988) showed that retinal progenitor cells can give rise to heterogeneous clones, but it was still unclear whether multipotency was a common feature of all retinal progenitors, or whether this potency became restricted with continuing progenitor divisions. Recent live-cell imaging techniques have shown that some late retinal progenitors may be programmed to produce specific combinations of retinal cells (Cohen et al., 2010; Gomes et al., 2011).

Adult retinal stem cells (RSCs) are rare pigmented cells in the ciliary epithelium at the retinal periphery of mice (Tropepe et al., 2000) and humans (Coles et al., 2004). RSCs proliferate in vitro to give rise to spheres of stem/progenitor cells and can differentiate into all retinal neural lineages, including photoreceptors, as well as retinal pigment epithelial (RPE) cells (Tropepe et al., 2000). While some labs have challenged the stem cell nature of the RSC (Cicero et al., 2009; Gualdoni et al., 2010), others have confirmed RSCs as stem cells (Coles et al., 2004; Ahmad et al., 2000; Abdouh and Bernier, 2006; Inoue et al., 2010; Demontis et al., 2012; Del Debbio et al., 2013; Fang et al., 2013). One lab has argued a transdifferentiation origin for RSCs (Cicero et al., 2009); however, this is unlikely given the ability to prospectively enrich a rare clonal population from the ciliary epithelium with stem cell properties (Ballios et al., 2012). Transdifferentiation is defined as the conversion of one differentiated, non-stem cell type directly to another differentiated cell type, and has been demonstrated in the retina of amphibians as well as embryonic chick and rat by manipulation of exogenous growth factors (Park and Hollenberg, 1989; Opas and Dziak,

---

1994). Prospective enrichment of a clonally proliferative and multi-potent retinal stem cell based on the criteria of size, pigmentation and P-cadherin levels (Ballios et al., 2012) suggests that transdifferentiation is an unlikely mechanism to describe these results. Additionally, in both Chx10-null and Mitf-null mice with reduced neural retinal and RPE progenitor populations, respectively, a 3–8 fold increase of RSCs was observed (Coles et al., 2006). If this was due to ciliary epithelium-transdifferentiation, then in the Mitf-mutant, fewer pigmented epithelial cells should be available for transdifferentiation into RSCs.

We previously found that combinations of taurine (T), retinoic acid (RA), Fibroblast Growth Factor 2 (F) and heparin (H) (T + RA + FH) added to differentiating clonal RSC colonies increases the number of rods to 90% of all progeny (Demontis et al., 2012; Bassett and Wallace, 2012). These terminally-differentiated cells show no evidence of pigmentation by electron microscopy and display multiple markers of mature rod photoreceptors (Ballios et al., 2012). The time courses for the expression of immature (Neural retina leucine zipper, Nrl+) and mature (Rhodopsin+) rod markers by RSC-derived rods closely follow the profile of Nrl/Rhodopsin expression during rod development in vivo (Akimoto et al., 2006), suggesting adult RSC-derived rods in vitro may pass through a similar intrinsic differentiation program as newborn rods in vivo. In this study, we investigated the hypothesis that T + RA acts directly on early RSC progeny in an instructive, rather than permissive manner, to bias photoreceptor differentiation through the enrichment of rod-specific progenitors.

Several studies have suggested that the cone fate may be a default pathway of photoreceptor development (Akimoto et al., 2006; Mears et al., 2001; Brzezinski and Reh, 2015; Szel et al., 1994). For example, deletion of Nrl leads to the complete loss of rod function with normal cone function, mediated by short-wavelength or S-cones (Mears et al., 2001). Likewise, retinoid-related orphan receptor β (RORβ, a rod and cone differentiation regulator) knockout mice lack rods and show an excess of S cone-like photoreceptors, recapitulating the effects seen in $Nrl^{-/-}$ mice (Swaroop et al., 2010). Finally, studies on the ontogeny and evolution of photoreceptors suggest that the S-cone represents an evolutionarily older form of photoreceptors (Szel et al., 2000; Kim et al., 2016). To study whether S-cone is a default pathway for retinal progenitors, we used COCO, a Cerberus/Dan family member that inhibits BMP, Nodal/TGFβ and Wnt signaling pathways to block other retinal cell fates. COCO has been previously used to induce the differentiation of human embryonic stem cells into cone photoreceptors, and has been shown to be a powerful neural and photoreceptor inducer (Zhou et al., 2015). The cell biological mechanisms underlying the production of cone photoreceptors by COCO are not known, but we hypothesize that it may instruct lineage decisions in retinal progenitors by suppressing alternative non-cone cell fates.

2. Material and methods

2.1. Animals

The mice used in these studies for isolation and characterization of RSCs and RSC-derived rod and cone photoreceptors include C57BL/6, *Actin.gfp* (This transgenic mouse line, with an "enhanced" GFP (EGFP) cDNA under the control of a chicken beta-actin promoter and cytomegalovirus enhancer, has widespread EGFP fluorescence, with the exception of erythrocytes and hair), *Actin.yfp* (constitutively express YFP in all cells) and CCDC $136^{-/-}$ mice (Smiley et al., 2016b). Experimental procedures were performed in accordance with the Guide to the Care and Use of Experimental Animals and approved by the Animal Care Committee at the University of Toronto.

2.2. Cell culture

RSCs were derived from the ciliary epithelium of adult mice (male and female, minimum 6 weeks old), or from E14 presumptive ciliary marginal zone epithelium, as described previously (Coles et al., 2006). Neural retina progenitors were derived from the neural retina tissue of the E14. Cells were plated in serum free media (SFM) on non-adherent tissue culture plates (Nunc; Thermo Fisher Scientific) at a clonal density of 10–20 cell/μL + Fibroblast Growth Factor and Heparin.

2.3. Differentiation

For differentiation, individual RSC spheres were selected after 7 days of primary culture. Spheres were derived from *Actin.gfp* mice to confirm appropriate sub-cellular localization of protein products on immunofluorescence and spheres from C57BL/6 were picked on average 80–100 μm. Spheres (1–2/well) were plated on laminin (50 ng ml^{-1}, Sigma)-coated 24-well plates (Nunc). Following four days of culture in SFM plus FGF2 (10 ng ml^{-1}, human recombinant; Sigma) and heparin (2 ng ml^{-1}; Sigma) to encourage sphere adhesion and spreading, the media was replaced with the rod-induction media (refreshed every four days): SFM plus taurine (100 μM; Sigma), retinoic acid (RA) (500 nM; Sigma), FGF2/heparin (FH), as described previously (Ballios et al., 2012). Pan-retinal differentiation media includes 1% FBS (Invitrogen, Burlington, ON) and FGF2/heparin. For cone differentiation: Pan-retinal conditions + COCO 50 ng/mL (R&D Systems 3356-CC) were used for 28 or 45 days. COCO was added from day 0 of the differentiation. For experiments involving sonic hedgehog signaling blockade, cyclopamine (1 μM; Toronto Research Chemicals, Inc.) was added beginning at either 0 days or 14 days of differentiation according to the schema outlined in Fig. 5, A. Cyclopamine dose was based on dose-response for pan-retinal cell survival at 14 days of differentiation (data not shown).

2.4. Immunostaining

Cells were rinsed with PBS, followed by 4% paraformaldehyde for 10 min at room temperature. Cells were permeabilized with 0.3% Triton X-100 for 10 min and pre-blocked with 5% normal goat serum for 1 h at room temperature. Primary antibodies, rabbit anti-cone arrestin (AB15282, 1:2000; millipore), rabbit anti-S-opsin (Ab81017, 1:100; Abcam), mouse anti rhodopsin (MAB5316, RetP1, 1:250; Millipore), mouse anti RPE65 (MAB5428, 1:250; Millipore), mouse anti-Pax6 (1:400; Developmental Studies Hybridoma Bank, Iowa City, IA), PKC (ab19031, 5 μg/mL), MITF (ab12039, 1 μg/mL), mouse anti-CRALBP (1:500; Abcam, Cambridge, MA), mouse anti-calbindin (1:500; Sigma) and Rhodamine peanut agglutinin (RL-1072, Vector laboratories) were reacted for 1 h at room temperature or overnight at 4 °C. Samples then were incubated with Alexa Fluor secondary antibodies conjugated with Alexa488, Alexa568, or Alexa647 (all 1:400) (Life Technologies) for 1 h at room temperature. Nuclei were stained with Hoechst dye 33,258 (Sigma) (Bazhulina et al., 2009). Cell staining was examined under a fluorescence microscope (Axio Observer D1; Carl Zeiss) with AxioVision 4.8 software (Carl Zeiss).

2.5. Retroviral clonal labeling

Proliferating RSC progeny were labeled using a GFP-expressing retrovirus 12 h after plating in rod differentiation or pan-retinal differentiation conditions. Retrovirus was prepared as previously described (Holowacz et al., 2011). Concentrated aliquots of virus from a single stock were serially diluted in SFM immediately before use. A dilution of approximately one viral particle per well reliable produced 0-to-1 labeled clone. Media was changed after 48 h. Cells were fixed and clones analyzed by immuno-staining at 28 days of differentiation (a time sufficient to produce mature, post-mitotic, RSC-derived rods (Ballios et al., 2012)). Clone survival rates were calculated taking into account the plating efficiency in terms of the number of wells with single cells at 16 h post-FACS, and the survival of those clones at the end of differentiation.

2.6. Flow cytometry, sorting and labeling cells

For pigmentation sorts, RSCs spheres were dissociated into single cell and cells were sorted based on forward and side scatter without the use of surface markers using a FACS Aria (BD Biosciences) (Fig. S2 A–D) (Ballios et al., 2012). Cells were counterstained with propidium iodide (0.9 μg μl^{-1}, Invitrogen) to assess viability. Analysis was performed using BD FACS Diva Software V6.1.2. Single cell/well sorts were performed into 96 well clear-bottom plates (Nunc), coated with laminin. 14% of single cells survived dissociating and sorting, and 50–70% of those clones were present by the end of the experiment, showing that clones in approximately 7–10% of wells initially plated survived until the end of the experiment. When defining a pigmented population of cells from the sphere for sorting, a population of cells with high SSC was chosen by comparison to control neural retina samples (which do not contain pigmented cells). This sort was displayed by plotting against a second, empty channel (FITC) as is standard practice. Cells exhibit some autofluorescence in the FITC spectrum, but were not specifically stained with any fluorescent-tagged antibodies, or sorted based on this. For cone photoreceptor isolation and sort, neural retina tissue was harvested and dissociated into single cell using a Papain kit (Worthington #LK003150). Cone photoreceptors first labeled with peanut agglutinin (PA), a cone specific marker, and then doubled sorted for both GFP and Rhodamine Red.

2.7. Quantitative RT-PCR

RNA was extracted using NORGEN BIOTEK RNA extraction kit (Cat# 35300) with DNase to remove genomic DNA contamination. RNA was quantified using Nanodrop and a specified amount of cDNA was reverse-transcribed using Superscript III (Invitrogen#18080-051). PCR was carried out using standardized TaqMan Gene Expression Assays in a 7900HT Fast Real-Time PCR System (Applied Biosystems). Quantification was performed using the delta Ct method with Hprt, Beta actin or Gapdh as an endogenous control, and neural retina tissue as calibrator.

2.8. RNA sequencing

The transcriptome of 3 groups (and 3 independent biological experiment in each group): CCDC-RSCs, CCDC-COCO-cones, and CCDC-endogenous cones were compared. CCDC 136$^{-/-}$ mice express GFP in their cone photoreceptors (Smiley et al., 2016b). We took advantage of GFP marker to purify endogenous cones and RSC-derived cones from CCDC 136$^{-/-}$ mice for FACS (Fig. S2 B and C). High quality total RNA (RIN: 9–10) was subjected to directional RNA-sequencing library construction from three independent biological replicates. Sequencing was performed using GAIIx (Illumina, Inc., San Diego, CA; www.illumina.com). FASTQ files were generated from reads passing Chastity filter and analyzed for differential expression and PCA analysis.

2.8.1. Correlation at pathway activity level

We employed the BioConductor package of Gene Set Variation Analysis (GSVA) with the ability to perform pathway analysis on individual samples. GSVA was performed using the CPM-normalized and log2-transformed gene expression values of all samples with the following pathway gene set database: Mouse_GOBP_AllPathways_no_GO_iea_October_01_2016_symbol.gmt (Merico et al., 2010; Hänzelmann at al., 2013). GeneSet size was limited to a range of 10–200 genes.

GeneSet size was limited to range 10–200. 2000 permutations were carried out. Using the gmt file and same parameters as for GSEA the pathway activities of each cone samples in our study was calculated. The rank file generated for the reference dataset was used for GSEA calculation and served as reference in correlation analysis.

Table 1
The top 20 differentially express genes in RSC spheres vs. RSC-derived cones.

Genes	LogFC	Rankscore	PValue	FDR
Dct	11.59	4.49	3.27E-05	2.00E-03
Slc26a4	9.74	8.1	8.01E-09	3.26E-05
Tmem132d	9.65	7.71	1.94E-08	4.74E-05
Rgr	9.59	7.28	5.30E-08	7.20E-05
Tspan10	9.43	5.25	5.63E-06	9.17E-04
Lypd6b	9.42	7.53	2.95E-08	5.15E-05
Gsta2	9.34	5.37	4.27E-06	8.16E-04
Cyp1a1	9.02	6.01	9.82E-07	3.43E-04
Dpp4	8.76	6.17	6.72E-07	3.04E-04
Lgi1	8.69	6.65	2.25E-07	1.37E-04
Calcb	8.65	6.96	1.09E-07	9.81E-05
Tie1	8.57	6.81	1.54E-07	1.01E-04
Myrip	8.27	6.05	9.01E-07	3.42E-04
Mlana	8.26	8.16	6.97E-09	3.26E-05
Dmp1	8.22	4.38	4.17E-05	2.26E-03
Sv2b	8.05	8.77	1.69E-09	2.06E-05
Krt8	8.01	4.68	2.09E-05	1.68E-03
Ttr	7.99	4.59	2.55E-05	1.86E-03
Ctss	7.96	4.9	1.27E-05	1.37E-03
Tmem27	7.67	5.04	9.10E-06	1.18E-03
Cyp2f2	−12.17	−2.93	1.17E-03	1.32E-02
Kera	−12.12	−2.68	2.09E-03	1.90E-02
Dpt	−11.82	−3.13	7.41E-04	9.92E-03
Ddx3y	−11.54	−3.85	1.42E-04	4.05E-03
Pi15	−10.97	−2.65	2.25E-03	1.98E-02
Eif2s3y	−10.57	−3.59	2.56E-04	5.63E-03
Fgf10	−10.17	−2.97	1.08E-03	1.25E-02
Uty	−9.82	−3.92	1.20E-04	3.71E-03
Kdm5d	−9.78	−3.73	1.85E-04	4.70E-03
Xpnpep2	−9.43	−3.4	3.99E-04	6.92E-03
Sfrp2	−8.73	−2.07	8.57E-03	4.70E-02
Tnn	−8.65	−2.37	4.23E-03	2.99E-02
Sfrp4	−8.39	−2.78	1.66E-03	1.67E-02
F830016B08Rik	−8.12	−3.22	5.99E-04	8.70E-03
Apod	−8.03	−2.68	2.07E-03	1.88E-02
Myh15	−8.03	−2.73	1.85E-03	1.78E-02
Osr2	−7.66	−2.7	1.98E-03	1.83E-02
Rxfp1	−7.63	−2.56	2.73E-03	2.25E-02
Omd	−7.53	−2.53	2.93E-03	2.37E-02
Chodl	−7.44	−3.05	8.99E-04	1.12E-02

2.8.2. Determining differentially expressed (DE) genes and ranks

The standard method in the EdgeR software, Quasi-likelihood F-test, was used for DE determination in edgeR, because we have the minimal number of samples required (minimum 4 samples total and at least 2 per group) and it is more stringent than the classical and likelihood ratio methods. The ranking score for each gene is generated by p-values and fold changes from the analysis with the following formula:

$$\text{Sign (logFC)} \times -\log_{10}(\text{p−value})$$

Sign (logFC) determines the direction of the change with +ve as up-regulation and −ve as down. −$\log_{10}$(p-value) determine the scale of ranking, the lower the p-value, the higher the score. The genes are ordered from top up-regulated to down-regulated ones as rank files.

2.8.3. Lists of differentially expressed genes

DE genes from all 3 comparisons with false discovery rate or FDR q-value < 0.05 are listed and ranked by logFC (log 2 of Fold Change). The tables include logFC, rank scores, p-values, and FDR q-values. Top 20 regulated genes are listed here for each comparison. In each comparison we compared two types of cells, the genes are labeled in black for one cell type and blue for the other.

Total 3 comparisons are: 1) Endogenous Cone vs COCO Cone (Table 1); 2) CCDC-RSC vs COCO Cone (Table 2) and 3) CCDC-RSC vs Endogenous Cone (Table 3).

Table 2
The top 20 differentially express genes in RSC spheres vs. endogenous cones.

Genes	LogFC	Rankscore	PValue	FDR
Tspan10	10.4432427	16.1586498	6.94E-17	5.58E-15
Ttr	10.3087045	15.776313	1.67E-16	1.13E-14
Slc26a4	10.1827813	15.5438996	2.86E-16	1.74E-14
Dct	10.0358862	19.2012938	6.29E-20	2.85E-17
Tie1	9.01111536	12.710142	1.95E-13	4.42E-12
Ctss	8.58186018	13.0004954	9.99E-14	2.47E-12
Rgr	8.56649697	12.4708177	3.38E-13	7.09E-12
Sv2b	8.51907534	18.1884909	6.48E-19	1.57E-16
C1qa	8.45905406	11.4799513	3.31E-12	4.90E-11
Gsta2	8.43424768	17.3848417	4.12E-18	5.86E-16
Krt8	8.13444342	14.5603696	2.75E-15	1.18E-13
Slc4a5	8.00016679	20.2036869	6.26E-21	7.96E-18
Pld5	7.93656486	17.0157094	9.64E-18	1.11E-15
C1qb	7.87732224	10.0862462	8.20E-11	8.03E-10
Lgi1	7.51740836	10.5860699	2.59E-11	2.89E-10
Hkdc1	7.42516697	16.4772783	3.33E-17	2.97E-15
Myrip	7.41011002	9.99642575	1.01E-10	9.61E-10
Gucy2e	7.35547054	10.1974048	6.35E-11	6.42E-10
Tmem27	7.16000309	12.198696	6.33E-13	1.17E-11
Stxbp5l	7.09891972	13.4572497	3.49E-14	1.01E-12
Cyp2f2	−12.093933	−19.015194	9.66E-20	3.69E-17
Dpt	−11.991097	−19.943594	1.14E-20	1.07E-17
Pi15	−11.343474	−20.451256	3.54E-21	6.66E-18
Kera	−11.291784	−18.549153	2.82E-19	8.42E-17
Xpnpep2	−10.417263	−16.330386	4.67E-17	4.02E-15
Tnn	−10.103648	−16.727952	1.87E-17	1.84E-15
Fgf10	−9.8992156	−15.443936	3.60E-16	2.07E-14
Myh15	−8.7061324	−12.840425	1.44E-13	3.38E-12
Osr2	−8.6266181	−13.925633	1.19E-14	4.18E-13
Gdf6	−8.4556046	−13.952177	1.12E-14	4.00E-13
Fmo3	−8.387632	−11.998747	1.00E-12	1.74E-11
Tnfsf11	−8.3208991	−14.327896	4.70E-15	1.88E-13
Apod	−8.0655817	−19.535029	2.92E-20	1.88E-17
Sfrp4	−7.9567052	−12.612337	2.44E-13	5.32E-12
4833403I15Rik	−7.8724397	−12.459182	3.47E-13	7.25E-12
Bst1	−7.7909023	−12.008915	9.80E-13	1.71E-11
Kcnj15	−7.6961924	−13.740742	1.82E-14	5.81E-13
Crct1	−7.6528833	−11.076532	8.38E-12	1.09E-10
Itga11	−7.5503402	−13.473774	3.36E-14	9.85E-13
Gdpd2	−7.5291817	−13.521224	3.01E-14	9.04E-13

Table 3
The top 20 differentially express genes in endogenous cones vs. RSC-derived cones.

Genes	logFC	Rank score	PValue	FDR
Kdm5d	4.65	2.61	2.45E-03	1.26E-01
Eif2s3y	4.57	2.42	3.84E-03	1.46E-01
Uty	4.55	2.8	1.59E-03	1.10E-01
Ddx3y	4.13	2.41	3.90E-03	1.46E-01
Wnt9b	3.95	2.05	8.92E-03	1.91E-01
Dlk1	3.63	4.44	3.63E-05	4.62E-02
C1qb	3.6	1.72	1.92E-02	2.56E-01
Bex4	3.44	2.04	9.02E-03	1.92E-01
Sfrp2	3.41	1.08	8.25E-02	4.23E-01
Gm10800	3.06	2.03	9.24E-03	1.93E-01
Megf10	2.96	1.14	7.24E-02	4.06E-01
Gm21738	2.88	1.52	3.00E-02	2.94E-01
Erbb3	2.84	2.06	8.63E-03	1.89E-01
Cntn1	2.83	1.38	4.15E-02	3.35E-01
Ryr2	2.82	1.91	1.23E-02	2.17E-01
BC064078	2.79	1.96	1.09E-02	2.07E-01
Gm10801	2.78	2.21	6.22E-03	1.66E-01
Cwc22	2.78	1.76	1.74E-02	2.48E-01
Alpl	2.7	1.12	7.60E-02	4.12E-01
Khdrbs2	2.65	1.16	6.90E-02	4.00E-01
Crct1	−6.69	−3.65	2.23E-04	6.41E-02
Nefl	−5.99	−4.26	5.51E-05	4.62E-02
Rab3c	−5.81	−3.51	3.07E-04	6.70E-02
Col10a1	−5.56	−2.97	1.07E-03	9.94E-02
Xirp2	−5.22	−3.75	1.80E-04	6.41E-02
Aqp5	−4.75	−3.32	4.83E-04	8.43E-02
Myh2	−4.54	−3.57	2.70E-04	6.43E-02
Car8	−4.22	−2.94	1.16E-03	1.01E-01
Lrat	−4.21	−1.71	1.93E-02	2.57E-01
Sostdc1	−4.15	−2.78	1.65E-03	1.10E-01
Ivl	−4.06	−4.75	1.77E-05	4.62E-02
Cpa4	−4.04	−2.53	2.98E-03	1.35E-01
Myh11	−3.91	−2.98	1.04E-03	9.94E-02
Asb5	−3.79	−3.63	2.35E-04	6.41E-02
Bst1	−3.73	−1.64	2.29E-02	2.71E-01
Gm25911	−3.73	−3.15	7.02E-04	9.01E-02
Lce1h	−3.67	−2	9.93E-03	1.98E-01
Dgkk	−3.66	−3.37	4.22E-04	8.06E-02
Serpinb9b	−3.55	−2.47	3.39E-03	1.38E-01
Cyp1a1	−3.51	−2.58	2.65E-03	1.32E-01

2.9. Cell counts and statistics

All cell counts and pooled data are presented as averages with standard errors of the mean (SEMs). Statistics were performed using R (V 2.15.0) and Prism 5. Significance is noted using Student's *t*-test to compare two groups, or ANOVA when comparing three or more groups, with Tukey-Kramer post-hoc analysis (Bonferroni-adjusted p-values) for pairwise comparisons, where appropriate. Significance was noted for p-values < 0.05.

3. Results

3.1. RSC progeny can be biased towards rod or cone fates

In order to understand if early exposure to exogenous factors could bias RSC progeny fate, primary cultures of dissociated ciliary epithelium from adult mice were treated with T + RA + FH or FH-only during the standard 7-day sphere forming assay (14, 21). Our previous work showed that FH alone does not affect rod differentiation or pigmentation (Ballios et al., 2012). There was no difference in the number of clonal RSC sphere colonies (Fig. 1A), which were of similar size (99 ± 13 μm in FH-only vs. 103 ± 11 μm in T + RA + FH). Clonal RSC spheres are composed of both neural retinal (non-pigmented) and RPE (pigmented) progenitors (Coles et al., 2006). The pigmented progenitors lose their pigments in culture conditions while maintaining the expression of RPE markers such as MITF (Fig. S1B and C). Next, we used *Actin.yfp* mice, a transgenic mouse line with an "enhanced" YFP (EYFP)

with widespread YFP fluorescence. The advantage of using *Actin.*yfp cells is easier visualization of pigmented cells, as pigment absorbs YFP fluorescence. Thus, the degree of pigmentation in mixed spheres can be easily visualized. Spheres derived in T + RA + FH exhibited less pigmentation than FH-derived spheres, and thus may contain more non-pigmented progenitors than pigmented progenitors (Fig. 1C). When T + RA + FH-derived spheres (rod "lineage-primed" spheres) were differentiated in 1%FBS + FH for 40 days, the percentage of cells expressing Rhodopsin (a rod photoreceptor marker) was increased and RPE65 (a RPE marker) decreased compared to FH-derived spheres differentiated in 1%FBS + FH (Fig. 1B for quantitative data and Fig. 1E for immunocytochemical images). We and other groups have shown that RSC derived progeny treated with T+ RA express the Nrl and Rhodopsin genes (Demontis et al., 2012; Ballios et al., 2012), but do not express other retinal cell type specific genes (Ballios et al., 2012). There were no differences in total cell numbers of the minor populations expressing Pax6 (retinal progenitors and small numbers of differentiated amacrine cells), calbindin (interneurons), or CRALBP (Müller glia) (Fig. 1B). The increased number of rods arising from progenitors primed in T + RA at the expense of RPE differentiation suggests that these factors are instructive for the production of neural retinal progenitors during clonal RSC sphere formation, or at least critical for directing early lineage decisions between fate-restricted progenitors in vitro.

To evaluate the effect of COCO on adult RSC differentiation, we first tested different concentrations of COCO during the differentiation of clonal spheres derived from RSCs (Tropepe et al., 2000; Ballios et al.,
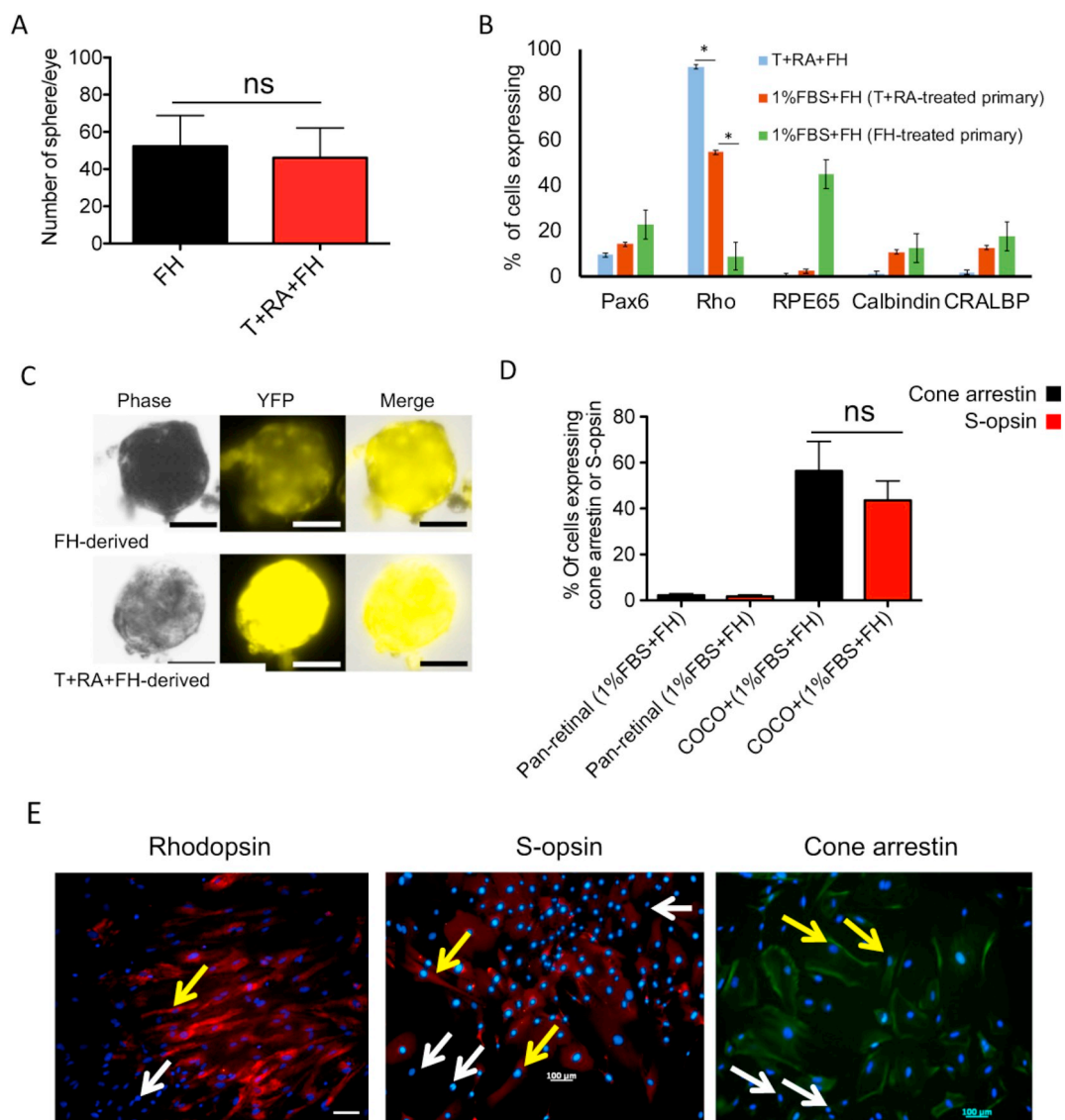
Fig. 1. Taurine and retinoic acid do not affect RSC sphere derivation from adult ciliary epithelium, but do shift baseline rod differentiation potential. COCO increases cone differentiation from RSC progeny. (A) No difference was found in the number of clonal RSC spheres derived from adult ciliary epithelium in standard growth media (FH) or with the addition of T + RA (t-test, p = 0.19). (B) Priming RSC progeny in T + RA shows a significant effect on neurogenic potential in pan-retinal differentiation conditions (1%FBS) assayed at 40 days, marked by a proportional shift from RPE (RPE65+) to rod photoreceptors (Rhodopsin+) (two-way ANOVA, interaction effect of cell type and differentiation condition on expression levels F $(8,50) = 12.81$, p = 0.0001; Tukey-Kramer post-hoc, p = 0.0001). Markers include Pax6 (retinal progenitors), Rhodopsin (rod photoreceptors), RPE65 (retinal pigment epithelium), calbindin (horizontal/off-bipolar cells) and CRALBP (Müller glia). The protocol for investigating neurogenic potential of RSC progeny "primed" in T + RA during RSC sphere derivation is illustrated. Scale bars represent 50 µm. Mean ± s.e.m. of n = 3 independent biological replicates. (C) Clonal RSC spheres derived in FH are a mixture of pigmented RPE progenitors and non-pigmented neural retinal progenitors. When derived in T + RA, the spheres show less pigmentation (indicated by less absorption of YFP signal in *Actin.yfp* cells) but a similar size (i.e., cell number), suggesting an asymmetric shift towards production of neural retinal progeny during RSC division. (D) Most RSC progeny treated with COCO throughout sphere growth and differentiation (and added to the 1% FBS + FH pan-retinal differentiation conditions) were positive for cone arrestin and S-opsin. In contrast, in pan-retinal differentiation conditions alone, RSC progeny produced < 1% cones. (E) Representative images of rhodopsin, S-opsin and cone arrestin (yellow arrows) expressing cells. Negative cells are shown with white arrows. The bisBenzimide H 33258, Hoechst stain, was used to visualize nuclei (blue) (39) (One-way ANOVA, F = 10.23, p = 0.0016). (For interpretation of the references to colour in this figure legend, the reader is referred to the web version of this article.)

2012). We found that a 50 ng/mL or higher concentration of COCO (+FH + 1%FBS) induced cone differentiation to approximately 60% of RSC progeny during a 28-day differentiation period, measured by cone arrestin expression, a mature marker of cone photoreceptors (Fig. S1A). Furthermore, protein kinase (PKC), a bipolar cell marker, was not expressed or detected in cells cultured in COCO conditions (Fig. S1D and E). In pan-retinal differentiation conditions (1% FBS + FH) alone, RSC progeny produced < 1% cone arrestin positive cells (Fig. 1D). In contrast, following 28 days of COCO treatment (COCO +1%FBS + FH), 56% of RSC progeny were positive for cone arrestin (Fig. 1D) and 46%

were positive for S-opsin (Fig. 1D). Given that the commercial primary antibodies that were available to co-stain the COCO-derived cells for both of these markers were from the same species, we instead tested whether there were any differences in the expression levels of cone arrestin versus S-opsin (Fig. 1E). Immunofluorescence staining of S-opsin and cone-arrestin expressing cells are shown in Fig. 1E. None of the cells positive for these cone markers co-stained for Rhodopsin or RPE65 (data not shown). Important, similar to previous studies (Demontis et al., 2012; Sparrow et al., 1990), we observed both in vitro rods and cones like-cells in two-dimensional cultures develop processes,
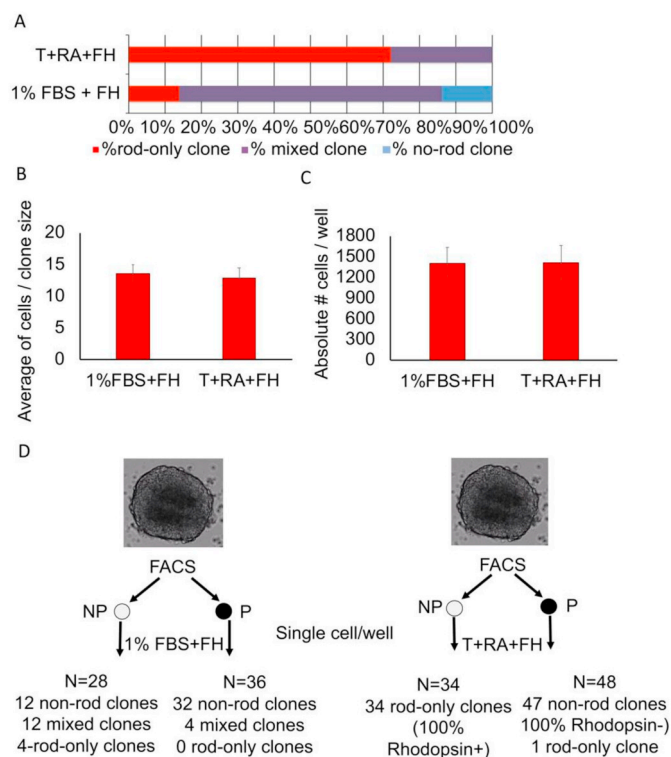
Fig. 2. Distribution of retinal progenitor clones in retroviral lineage tracing shows a bias towards mixed clones of high percentage rhodopsin + cells when differentiated in taurine and retinoic acid. (A) Clonal lineage analysis was performed in vitro by infecting differentiating cultures with a limiting dilution of replication-incompetent GFP retrovirus, such that only one cell per well was labeled at day 1. The composition of clones was analyzed after 44 d of differentiation. There was a large enrichment of rod-only clones present in T + RA cultures compared to pan-retinal differentiation conditions (1%FBS + FH). (B and C) The average clone size (t-test, p = 0.31) and the absolute number of cells/well (t-test, p = 0.24) in both conditions at 44 d of differentiation was similar. Means ± SEMs of > 40 clones in each condition across n = 3 independent biological replicates. (D) Single-cell per well analysis revealed that clones derived from non-pigmented progenitors in 1%FBS + FH were composed of mixed and no-rod clones, with a minority of rod-only (100% Rhodopsin +) clones. Those derived from pigmented cells were mostly no-rod clones, with only a minority of mixed clones. In T + RA, all clones derived from non-pigmented progenitors were rod-only clones, while those derived from pigmented progenitors were predominantly no-rod clones (no Rhodopsin + cells).

but do not elaborate an outer-segment like structures (Demontis et al., 2012; Ballios et al., 2012; Sparrow et al., 1990; McUsic et al., 2012; Ballios et al., 2015). However, scaffolds in three-dimensional cultures help photoreceptors develop outer-segment like structures (McUsic et al., 2012).

3.2. T + RA instruct RSC progeny to rods and COCO to cones

Two clonal approaches were used to investigate the possibility that T + RA + FH can encourage the specification of rod-specific progenitors. A fluorescent retroviral construct at limiting dilutions in vitro, allowed visualization of RSC progeny clones derived from single RSC-derived progenitors. Clonality was achieved using limiting dilutions to give a virus titer that infected < 1 cell/well. Clone composition was divided into three categories: clones in which there were all Rhodopsin + cells (rod-only clones), mixed clones, and no Rhodopsin + cells (non-rod clones). Comparisons of the frequency and character of clones fated for Rhodopsin-expression revealed enrichment in the percentage of rod-only clones between 1%FBS (13% of all clones) and T + RA (over 70%

of all clones), without any effects on the survival of clones, the numbers of cells per clone or the total numbers of cells per well (Fig. 2A and B and C) (> 40 clones in each condition, n = 3 independent biological replicates). This strongly argues against selective survival effects on rod progenitors or differential survival of post-mitotic rods within a clone as mechanisms for producing the increase in rod-only clones. Most interesting, when analyzing the composition of the individual mixed clones in both conditions (Fig. 3B and C), we found that mixed clones in T + RA + FH conditions were predominantly Rhodopsin+ (> 80% of cells in the clones), while those in 1%FBS + FH conditions were only 10–20% Rhodopsin+, consistent with those values seen at the population level(Ballios et al., 2012).

A second approach to analyze the cell biological mechanisms underlying rod progenitor specification made use of fluorescence-activated cell sorting (FACS) of dissociated, undifferentiated clonal RSC progeny. We sorted single non-pigmented or single pigmented retinal progenitors per well (see Methods), which were then treated with 1% FBS, T + RA, or T + RA + 1%FBS for 28 days of differentiation (Fig. 2D). In pan-retinal differentiation conditions (1% FBS), clones derived from non-pigmented progenitors were distributed between non-rod and mixed clones, with a minority of rod-only clones (100% Rhodopsin-positive; n = 4 of 28 clones) (Fig. 2D). Clones derived from pigmented cells in pan-retinal differentiation conditions never gave rise to rod-only clones, and only a minority of the clones were mixed. In T + RA conditions, all clones derived from non-pigmented progenitors (n = 34) were rod-only clones (100% Rhodopsin-positive), while those derived from pigmented progenitors (n = 47 of 48 clones) were almost all non-rod clones (Fig. 3A). Of note, one rod-only clone was derived from a single pigmented cell in T + RA conditions (the largest of the pigmented cell-derived clones in T + RA conditions with 20 cells), suggesting potential neural lineage plasticity in very early pigmented progenitors (which may explain the decreased pigmentation within T + RA treated clonal RSC spheres – Fig. 1C). Similar to T + RA treatment, in T + RA + 1%FBS all clones derived from non-pigmented progenitors (n = 34) were rod-only clones, while all those derived from pigmented progenitors (n = 48) were no-rod clones (Fig. 3A). Clone sizes were similar among the groups, although the addition of FBS did produce a non-significant trend to bigger clones (Fig. 3A). Survival rates of single cell clones one day after plating were similar between non-pigmented single cell clones in T + RA (7.0%), 1%FBS (8.9%) and T + RA + 1%FBS (10.2%); these single cells then proliferated to produce clones. These findings suggest that T + RA may instruct the early neural retinal progenitors produced by RSCs to become rod-specific progenitors in vitro.

Next, we explored the cell biological mechanism underlying cone progenitor specification. We again sorted undifferentiated clonal RSC progeny into single non-pigmented or pigmented progenitors, plated them at single-cell-per-well density and differentiated the clones in COCO or pan-retinal control conditions for 28 days. We found that only clones from non-pigmented progenitors (all 47 clones) in COCO contained cone arrestin positive cells. Interestingly, smaller sized clones (< 100 cells, n = 10 clones) were 100% cone arrestin positive. The larger clones were between 86%–96% cone arrestin positive (n = 37) after 28-days of differentiation (Fig. 3D; only clones < 600 cells are shown). All four groups exhibited similar average clone sizes, indicating that COCO does not cause differences in non-pigmented intra-clonal survival (Fig. 3E). Similar percentages of non-pigmented clones present at day 1 of plating survived to the end of the 28-day differentiation period in pan-retinal and COCO conditions, suggesting that COCO does not cause differences in inter-clonal survival (Fig. 3F). We hypothesize that during 28-day incubation with COCO, larger clones may still contain a majority of immature precursors, which do not yet express cone arrestin, or alternatively larger clones might be earlier progenitors that already have committed their earliest progeny to other retinal cell fates such as retinal ganglion cells and thus COCO may not have inhibitory effects on those specific cells. These data suggest that COCO
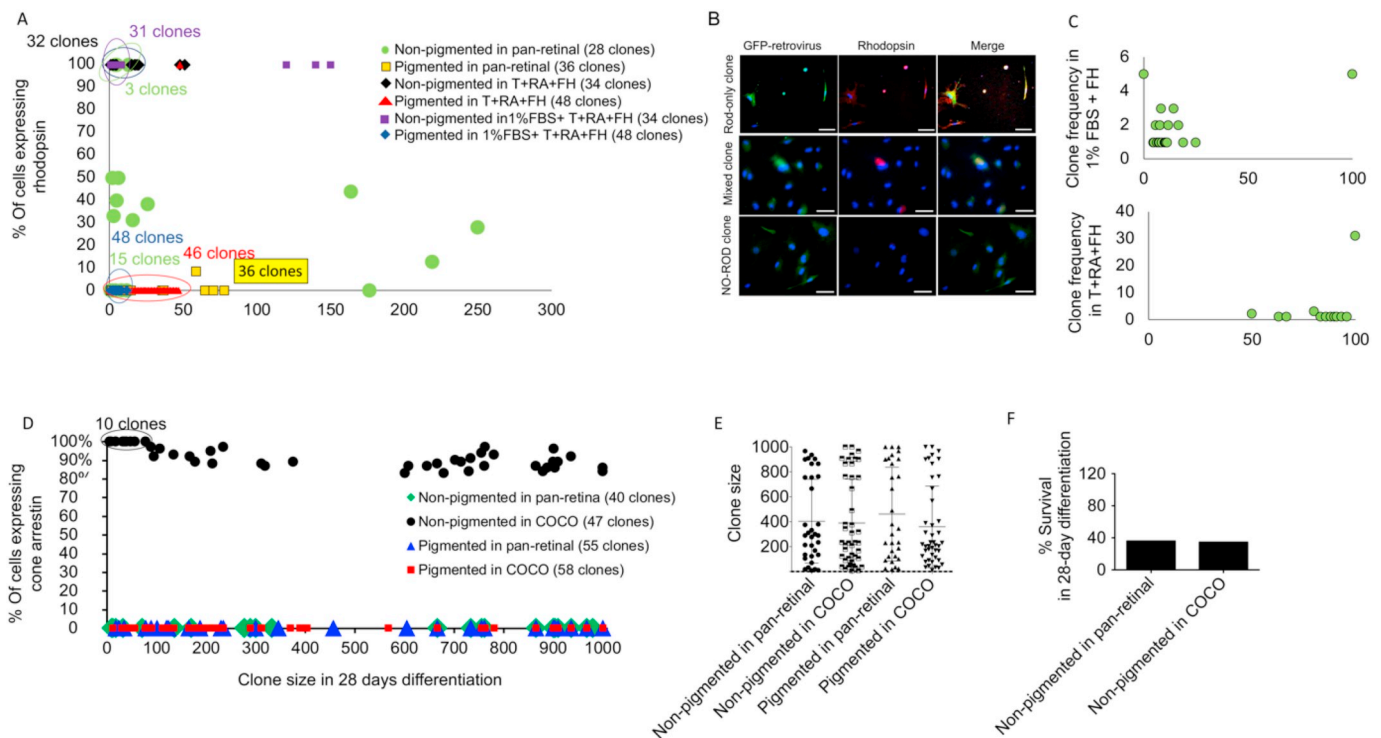
Fig. 3. Taurine and retinoic acid act instructively to generate lineage-restricted rod-specific progenitors while COCO suppresses other retinal cell fates and permits only cone photoreceptor differentiation. (A) The distribution of Rhodopsin + cells in clones of varying size in each of the analyzed clonal growth conditions is shown. A small number of clones > 1000 cells in size were excluded from this graph. These include 4 clones (> 1000 cells) from the 1%FBS + FH non-pigmented fraction (1 rod-only clone, 3 mixed with %Rhodopsin < 50%), and 3 clones (> 1000 cells) from the 1%FBS + FH pigmented fraction (1 non-rod clone, and 3 mixed with % Rhodopsin < 10%). The numbers placed above the counts represent the number of rod-only clones in that cluster derived from non-pigmented progenitors in T + RA (blue) and T + RA + 1%FBS (red), and non-pigmented progenitors in 1%FBS + FH (purple). Clone sizes were similar among the groups, as two-way ANOVA revealed no significant main effects of differentiation condition or pigmentation on clone size, and no significant interaction effect (F(2,234) = 2.41, p = 0.09). (B) Representative images of terminally differentiated clones labeled with GFP-retrovirus. Cells are stained for rhodopsin, showing rod-only, mixed and no-rod clones. Note, the morphology of RSC-derived progeny in vitro is diverse and does not correlate with the expression of rhodopsin in these cells. Hoechst stain is used to visual nuclei (blue). Scale bars represent 100 μm. (C) Mixed clones that underwent differentiation in pan-retinal conditions show a shift towards lower percentages of rhodopsin + cells (multiple mixed clones are 10–20% rhodopsin +) compared to clones differentiated in T + RA (multiple mixed clones are > 80% rhodopsin +). Data presented from > 40 clones in each condition across n = 3 biological experiments. (D) When single cells were exposed to COCO for 28 days, the large majority of non-pigmented clonal progeny were cone arrestin positive (all of the clones of < 75 cells were 100% cone arrestin positive). Pigmented progenitors did not produce any cones under COCO or pan-retinal conditions (One-way ANOVA, F = 0.8287, Tukey post-hoc test, p < 0.0001). (E) Clone size among the 4 different groups. Similar average clone sizes and thus survival between clones suggest that COCO may not cause differences in non-pigmented intra-clonal survival (F₃, ₈ = 0.828, p = 0.5143). (F) Similar percentages of non-pigmented clones present at day 1 of plating survived to the end of differentiation period in pan-retinal and COCO conditions suggesting that COCO does not cause differences in inter-clonal survival. Data represents means ± SEMs across n = 3 independent biological experiments (t-test, p = 0.321). (For interpretation of the references to colour in this figure legend, the reader is referred to the web version of this article.)

may act only on non-pigmented progenitors to produce cone specific progenitors in vitro.

3.3. Fetal and adult progenitors respond identically

To determine whether the rod lineage induction effects of T + RA observed with adult RSC-derived progenitors are applicable to the multipotent precursor cells that build the retina during development, we isolated clonal RSCs from the presumptive ciliary margin of 14 day-old embryos (E14), as well as neural retinal progenitor cells from the developing retina. This early embryonic time point was chosen before rods are normally produced in the developing retina, to test the hypothesis that exogenous factors also could instruct early embryonic retinal progenitors born in vivo. Cultures of clonal non-pigmented E14 neural retinal progenitor cells or E14 RSCs in T + RA for 28 days resulted in rod differentiation to > 90% of progeny, similar to adult RSC cultures (Fig. 4A). This reinforces the similarity between newborn progenitors from adult RSCs and early embryonic RSC-derived retinal progenitors. E14 RSC progeny was also subjected to a pulse of T + RA early in differentiation (a "lineage-priming" regime) similar to

experiments performed on early adult RSC progeny (Fig. 1B). In keeping with these results, E14 RSC progeny showed more biased rod differentiation when primary cultures were primed with T + RA (over days 0–3 only of 7-day sphere growth) and then differentiated in 1% FBS + FH for 28 days (Fig. 4B) compared to cultures not primed before differentiation. This propensity for lineage priming suggests that early retinal progenitors from developing retina show a similar readiness for instruction to a rod fate as those progenitors derived from the early asymmetric divisions of adult RSCs.

A similar result was obtained when clonal neural retinal progenitor spheres derived from E14 embryos were exposed to COCO during differentiation. Over 90% of E14 neural retinal progenitor cell progeny expressed cone arrestin and S-opsin when treated with COCO (Fig. 4C and D). < 5% of neural retinal progeny expressed cone arrestin in pan-retinal conditions (Fig. 4C and D). These data suggest that the effects of COCO on adult RSC-derived progenitors are similar to those on embryonic neural retina progenitors. Taken together, these data reinforce the similarity between newborn progenitors from adult RSCs and early embryonic retinal progenitors in culture conditions.
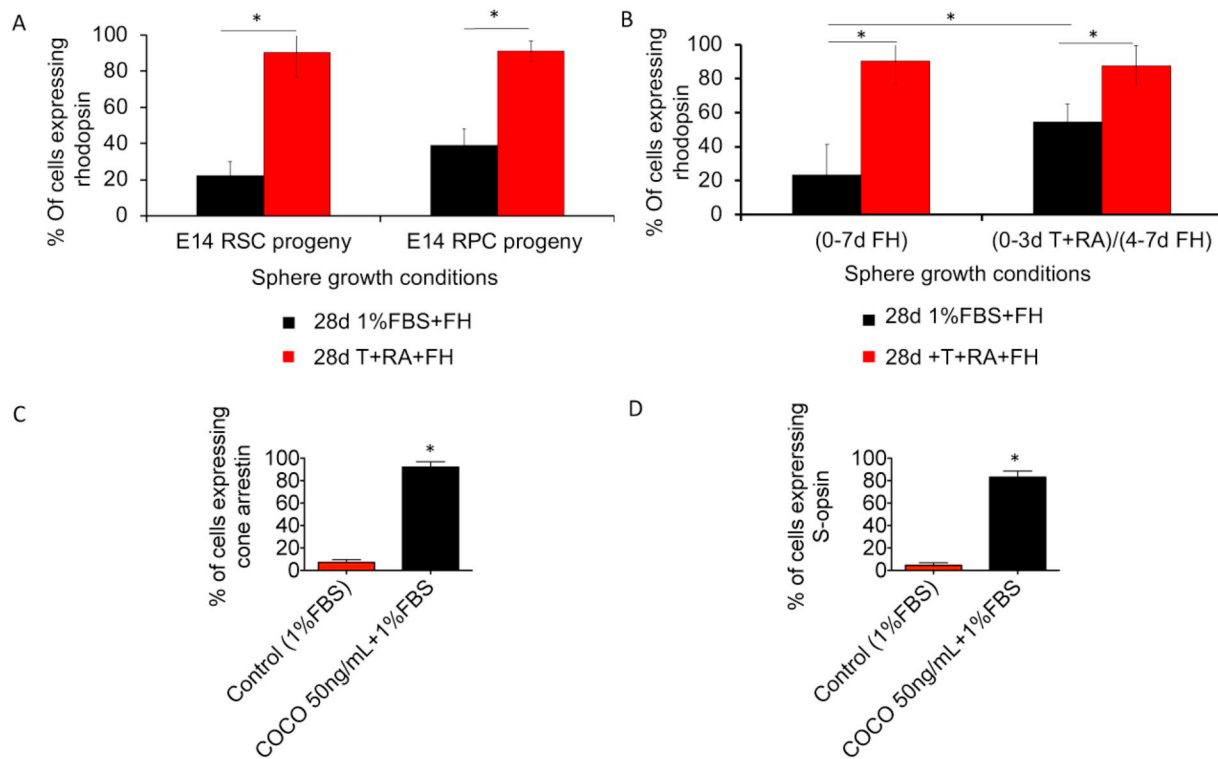
Fig. 4. E14 RSC or neural retinal progenitor spheres exhibit similar differentiation and rod-lineage priming effects of taurine and retinoic acid, and E14 neural retina progenitor spheres show similar cone differentiation patterns in COCO to RSC progeny. (A) Clonal E14 neural retinal progenitor cell (RPC) spheres were subjected to standard sphere growth conditions before differentiation for 28 days in pan-retinal or rod-inducing media. These neural retinal progenitors also showed enrichment for rod differentiation when subjected to T + RA compared to pan-retinal differentiation media. Two-way ANOVA revealed a significant interaction of cell type and differentiation conditions on Rhodopsin expression levels F (1, 17) = 6.95, p = 0.0003; Tukey-Kramer post-hoc, p = 0.0001. Means ± SEMs of n = 3 independent biological experiments. (B) RSC clonal spheres derived from E14 presumptive ciliary marginal zone epithelium were subjected to standard sphere growth conditions (0-7d FH) before differentiation for 28 days in either pan-retinal (1%FBS + FH) or rod-inducing (T + RA + FH) media. The enrichment of E14 RSC-derived rods demonstrates that T + RA also has a rod-inducing effect on progenitors derived from RSCs that are isolated during embryonic development from the growing eye. Cultures also were subjected to priming in T + RA (0–3d) at the start of clonal RSC sphere growth, and demonstrated rod enrichment in subsequent differentiation in pan-retinal conditions (1%FBS + FH), relative to RSC spheres that lacked priming. Two-way ANOVA revealed a significant interaction effect of sphere growth conditions (i.e., primed with T + RA, days 0–3 of initial sphere growth or not) and post-sphere differentiation conditions on percentages of cell expressing rhodopsin F (1,15) = 7.33, p = 0.0002; Tukey-Kramer post-hoc, p = 0.0001. Data represent means ± SEMs of n = 5 independent experiments. (C) Clonal non-pigmented spheres derived from E14 neural retina tissue were exposed to COCO or pan-retinal control differentiation conditions for 45 days. The vast majority of progeny in COCO were cone arrestin positive compared to 5% positive in pan-retinal conditions (*t*-test, p = 0.0001). (D) Neural retina spheres treated with COCO were largely positive for S-opsin, while < 2% were positive in pan-retinal control (t-test, p = 0.0001). Data represents means ± SEMs (* p < 0.05).

3.4. Sonic hedgehog regulates proliferation in the early progenitor expansion phase of RSC progeny differentiation

The sonic hedgehog (Shh) pathway increases the proliferation of retinal progenitors, while inactivation of Shh decreases the number of progenitors(Wall et al., 2009; Wang et al., 2005). We hypothesized that similar to retinal development, Shh signaling would be critical in the early progenitor expansion phase of RSC differentiation. Cyclopamine was used to antagonize hedgehog signaling in differentiating cultures (Fig. 5A). Blockade of Shh reduced the expansion of RSC-derived progenitors (decreased absolute numbers of cells and Ki67 staining by 50%, Fig. 5B and C, n = 3 independent biological replicates) specifically in the first two weeks of differentiation, with no effect on the percentages of cell phenotypes assayed at 2 or 6 weeks (Fig. 5D–G). This suggests that the composition of the progenitor pool, as well as rod fate specification, was unaffected. Taken together, these results demonstrate the double dissociation of two distinct processes in RSC differentiation: progenitor expansion by Shh and fate change by T + RA signaling.

3.5. T+ RA act on early retinal progenitors, while COCO is required throughout the differentiation

To confirm our hypothesis that the effect of T + RA on rod fate bias

was specifically on early progenitors, we subjected adult RSC progeny to pulses of T + RA in culture at progressively later time points in differentiation (Fig. 6A). Pulses of T + RA on late progenitors (11–14 days of differentiation versus 7–10 days of differentiation) in culture showed progressively decreased bias for rod differentiation with the later pulses (Fig. 6B), suggesting T + RA does not act instructively on late retinal progenitors to bias rod differentiation. Taken together with our earlier T + RA priming experiments (Fig. 1B) these data strongly argue against the selective survival of a late progenitor or post-mitotic cell as a mechanism for rod-enrichment within clones.

To investigate the temporal window during which COCO influences cell fate during differentiation, we treated RSC derived spheres with or without COCO at different time points throughout the differentiation period (first two weeks of differentiation, last two weeks of differentiation or the entire period of differentiation). > 50% of RSC progeny expressed cone arrestin and S-opsin only when cells were treated with COCO throughout the entire differentiation period (Fig. 6C). However, these cone markers were never detected when COCO was present only at the beginning or late in the differentiation period. Thus, COCO must be present throughout the 28-day differentiation period to bias cone production.
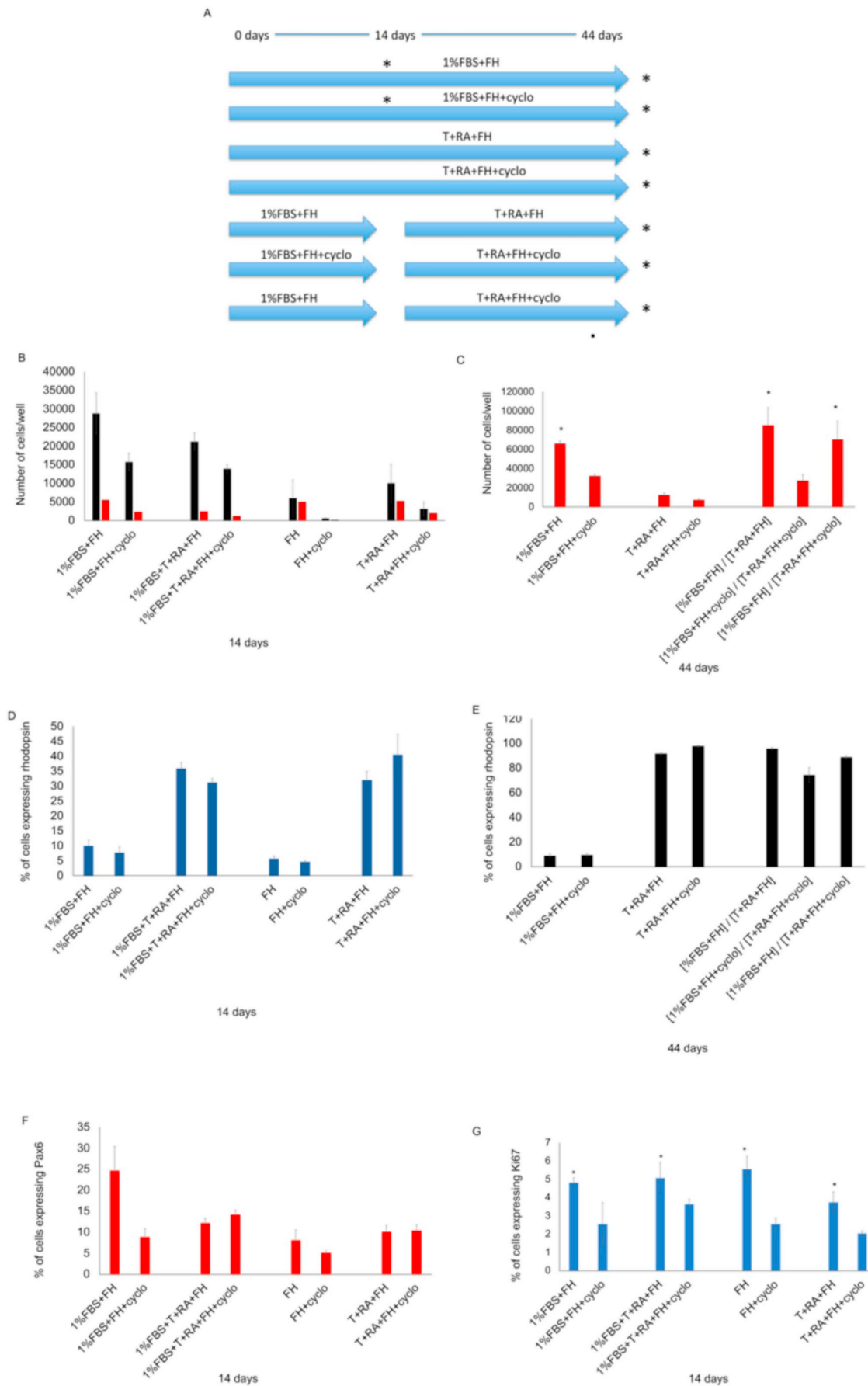
(caption on next page)

Fig. 5. Sonic hedgehog regulates proliferation in the early progenitor expansion phase of RSC progeny differentiation in T + RA. (A) Cyclopamine (Cyclo) was used to antagonize sonic hedgehog (Shh) signaling in differentiating cultures of RSC progeny according to this experimental schema. The effect of hedgehog blockade was evaluated in terms of absolute numbers of cells/well, expression of mature and progenitor cell markers (Rhodopsin and Pax6, respectively), and cell proliferation markers (Ki67). The first two weeks of differentiation are marked by significant proliferation under the influence of 1%FBS. * Represents time points for experimental analysis. Quantification of the absolute numbers of cells/well and the Rhodopsin expression in cultures at 14 (B and C and D) and 44 (C and E) days of differentiation. The overall proliferation in these cultures was decreased when cyclopamine was present in the first two weeks, specifically. This effect can be observed directly at 14 days in cultures treated with cyclopamine in (B), (Two-way ANOVA, main effect of sphere growth condition ($F(3,45) = 17.93$, $p = 0.001$), and main effect of cyclopamine ($F(1,45) = 14.91$, $p = 0.0003$), but no significant interaction effect ($F(3,45) = 0.62$, $p = 0.09$) on absolute numbers of cells/well, and C, (One-way ANOVA, shows an effect of condition ($F(6,31) = 30.08$, $p = 0.002$) on absolute numbers of cells/well; Bonferroni's post-hoc, $p = 0.02$). (D and E) Treatment with cyclopamine had no significant effect on rod phenotype in the immature (14 days) and mature cultures (44 days) (ANOVA analysis). (F and G) Quantification of Pax6 and Ki67 expression at 14 days showed a decrease in cell proliferation when cultures were treated with cyclopamine; in G Two-way ANOVA, main effect of cyclopamine, $F (1, 23) = 21.23$, $p = 0.003$. Means ± SEMs of n = 3 independent experiments.

3.6. RSC-derived cones exhibit similar transcriptomes to those of endogenous cones

To examine the overall gene expression similarities between adult RSC-derived cones and endogenous cones, we used adult CCDC136$^{-/-}$ mice, which express GFP specifically in cones and a sub-population of bipolar cells (Smiley et al., 2016a). To isolate only cones, we sorted both RSC-derived and endogenous cones for GFP and peanut agglutinin (a mature cone marker) (Fig. S2 B and C, see Materials and Methods) (Smiley et al., 2016a). Principal component analysis of RNA sequencing data revealed very similar transcriptomes of the adult RSC-derived cones to their endogenous counterparts (the adult stem cell derived cone transcriptome samples encircle the endogenous cone gene expression samples - Fig. 6D). Analyses of gene pathway activities are thought to provide a more robust measure of correlation between samples in RNA sequencing experiments. Therefore, using GSEA (gene set enrichment analysis), we performed pathway analysis on our endogenous and RSC-derived cones and correlated this with sequencing data of endogenous photoreceptors from a separate and independent reference database (Mo et al., 2016). These data show that both our endogenous and RSC-derived cones are highly correlated at the gene pathway level with the reference cones and not with reference rod photoreceptors (Fig. S3). 11 out of the top 20 differentially expressed genes were identical in endogenous and RSC-derived cones when compared to the starting RSC-derived sphere colonies, supporting the transcriptomic similarities between endogenous and RSC-derived cones (Tables 1 and 2). Additionally, the top 20 differentially expressed cone genes in Tables 1 and 2 had an average of 9-fold change (up-regulation), whereas the top 20 differentially expressed genes in Table 3 between endogenous and RSC-derived cones had an average of 4-fold change. Given the proposed similarities between endogenous and RSC derived cones, we would predict there to be smaller fold changes in their differential expression. The cone transcriptomes are clearly separated from the RSC-derived sphere transcriptomes (Fig. 6D). Moreover, the transcript of rod specific genes such as Rho, Nrl, Nr2E3, Rod arrestin, PDE beta and CNGB1 was not detected by RNA sequencing, suggesting specificity of cone photoreceptor enrichment during differentiation with COCO.

Due to sensitivity and specificity, we used qRT-PCR to validate the RNA Sequencing result. Retinal stem cell cone progeny showed high gene expression of Crx, cone arrestin (Arr 3), S-opsin and M-opsin only when cells were exposed to COCO throughout the entire differentiation period (Fig. 6E). Furthermore, Rho, Nrl, NR2E3 and GNGT1 (rod specific genes) were not detected in RSC-derived cones (Fig. 6E), while rod genes were present in T/RA induced rods (Ballios et al., 2012). Pax6 and Vsx2 were down regulated by the end of the differentiation periods, suggesting a loss of retinal multipotency (Fig. 6E). The effects of COCO on the differentiation of RSC progeny suggest that it act instructively to suppress alternate retinal fates throughout the differentiation period. Our results suggest that cones might be the default pathway for non-pigmented retinal progenitors consistent with previous studies (Mears

et al., 2001; Brzezinski and Reh, 2015; Szel et al., 1994) and that the continued suppression of instructive signals for other non-cone retinal fates may allow the production of large cone-only clones with similar transcriptomes to those of endogenous cones.

Finally, we exposed non-pigmented RSC progeny to both T + RA and COCO simultaneously during differentiation (Fig. 6F). The vast majority of post-mitotic cells expressed rod rhodopsin rather than cone arrestin. This reinforces our observation that T + RA acts in an instructive manner to bias rod fate, and does so despite the presence of COCO.

4. Discussion

4.1. COCO acts instructively to continually suppress alternate fates throughout the differentiation period

It may be informative to conceptualize rod and cone differentiation as possessing both "mechanisms" (instructive or permissive) and "modes" (lineage-restricted or lineage independent). A priori, three alternative models might explain how directed RSC progeny differentiation can produce rod or cone-enriched cultures (Fig. 7). Our results with clonal analyses of rod and cone differentiation after T + RA or COCO, respectively, argue for an instructive, rather than a permissive (i.e., selective survival) mechanism of differentiation, as the overall absolute cell survival as well as inter- and intra-clone survival did not vary among differentiation conditions. This makes the permissive Model 1 unlikely. Model 2 suggests that T + RA and COCO instruct the fate of multipotent progenitors at every division to produce rod or cone precursors, respectively. Indeed, this mechanism is consistent with the finding that COCO must be present throughout the differentiation period in a lineage independent fashion to inhibit more instructive signals from biasing differentiation towards alternative non-cone retinal fates and allowing the default to a cone cell fate (and thus support Model 2 for cone differentiation in COCO).

4.2. T + RA acid acts directly on RSC progeny in an instructive/ lineage-restricted manner

However, the results of the lineage priming experiments on rod differentiation suggest that the effect of T + RA is on early, not late, progenitors. If multipotent progenitors were maintained throughout T + RA-induced differentiation, then we would expect clones with at least a small number of Rhodopsin-negative cells in the single-cell-per-well differentiation assays. These results make Model 2 unlikely for T + RA induced rod differentiation. Our data satisfy all of the criteria for Model 3, suggesting an early effect of T + RA (on early retinal progenitor cells) in instructing the production of rod fate-restricted early proliferative progenitors, which divide symmetrically to produce rod-only clones. The single large clone consisting of all rod photoreceptors that came from a single pigmented cell may indicate an instructive effect on retinal stem cells themselves. However, the lack of a
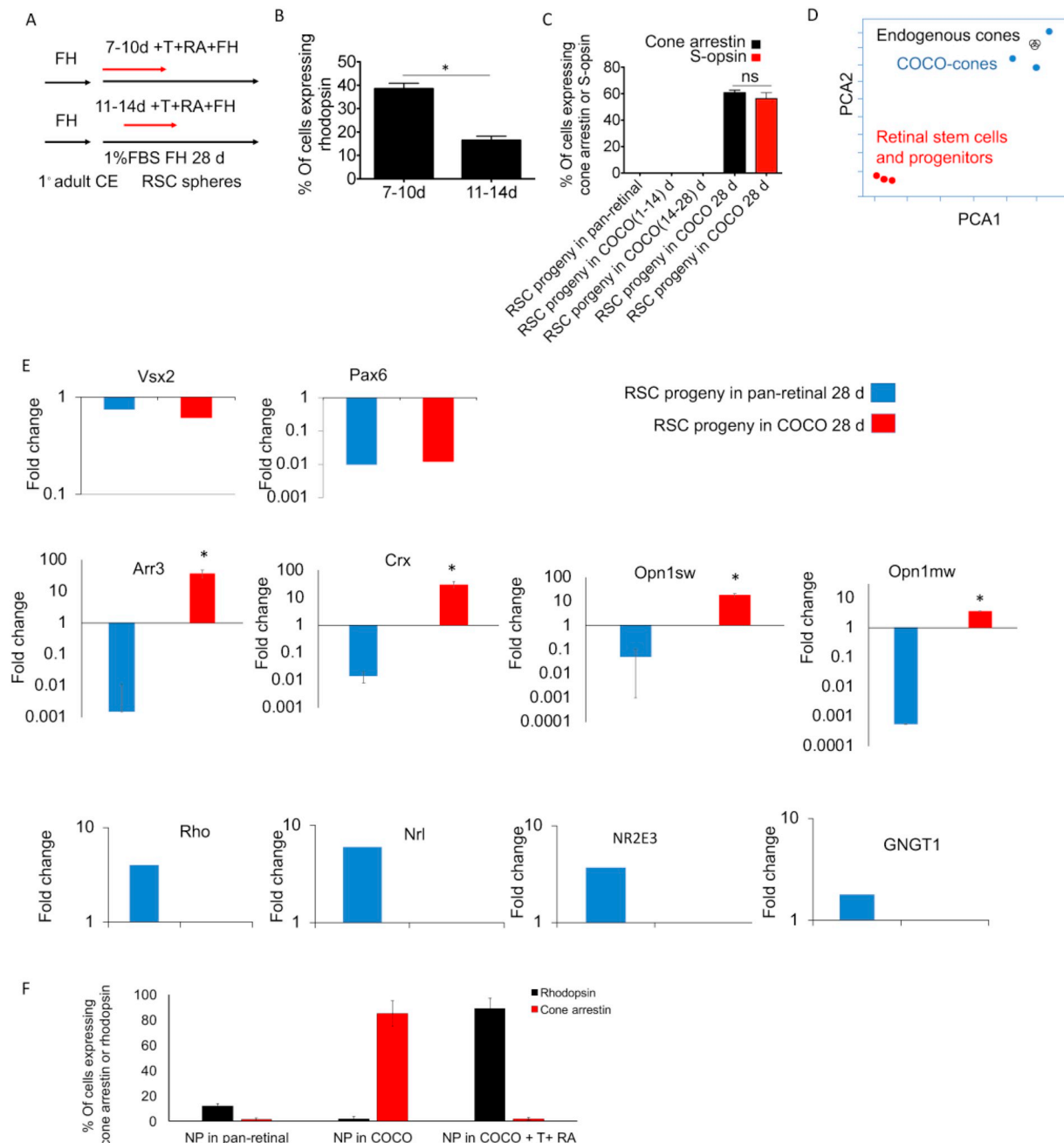
Fig. 6. Taurine/retinoic acid act instructively on early retinal progenitors to bias rod differentiation, while COCO is required throughout the differentiation period in order for RSC progeny to develop cone phenotypes with similar transcriptomes to endogenous cones. Rod differentiation outcompetes cone differentiation. (A) To test the effect of late pulses of T + RA exposure on rod lineage priming in RSC-derived progenitors, the schematic shows RSC-derived progenitors treated in pan-retinal conditions (1%FBS + FH) with 4 days of pulses of T + RA at 7–10 days and 11–14 days of differentiation. (B) T + RA is unable to bias rod fate when pulsed at later time points, demonstrating that the effect of T + RA on lineage priming of rod-restricted progenitors is likely an effect on relatively early progenitors, Means ± SEMs of n > 6 wells in each condition across n = 3 independent biological replicates (t-test, p = 0.001). (C) RSC progeny expressed cone arrestin and S-opsin only when cells were treated with COCO throughout the entire differentiation period (One-way ANOVA p < 0.0001). (D) Principal component analyses (PCA) of whole transcriptome data from undifferentiated clonal RSC colonies, RSC-derived cones and endogenous cones. The transcriptomes of adult RSC-derived cones clustered around their endogenous counterparts, and are distinct from the RSC-derived sphere transcriptomes. (E) RNA expression revealed that Crx (t-test, p = 0.003) and cone arrestin (Arr3) expression increased significantly (t-test, p = 0.0027) when RSC progeny were treated with COCO throughout the entire differentiation period compared to pan-retinal differentiation conditions. The expression of M and S opsin markedly increased under COCO differentiation conditions (t-test, p = 0.007). On the other hand, Pax6 and Vsx2, retinal precursor genes, were decreased at end of differentiation. Data represent means ± SEMs of n = 3 independent biological replicates. (* p < 0.05). (F) Non-pigmented RSC progeny were differentiated in pan-retinal conditions, COCO, or a combination of COCO and T + RA simultaneously for 45 days. Cells exposed to COCO alone expressed cone arrestin. On the other hand, cells differentiated under the combination of COCO + T + RA expressed rhodopsin. We suggest that COCO may serve to instruct a cone fate by suppressing instructive signals for other non-cone retinal fates, and is overwhelmed by the additional presence of exogenous T + RA. However, it also may be that T + RA act intracellularly, and thus the effect of T + RA on promoting rod fate in the presence of COCO inhibition may simply be the result of T + RA action downstream of COCO inhibition at the cell membrane receptor. Nevertheless, these findings emphasize that COCO must be active continuously to block other extracellular instructive differentiation signals.
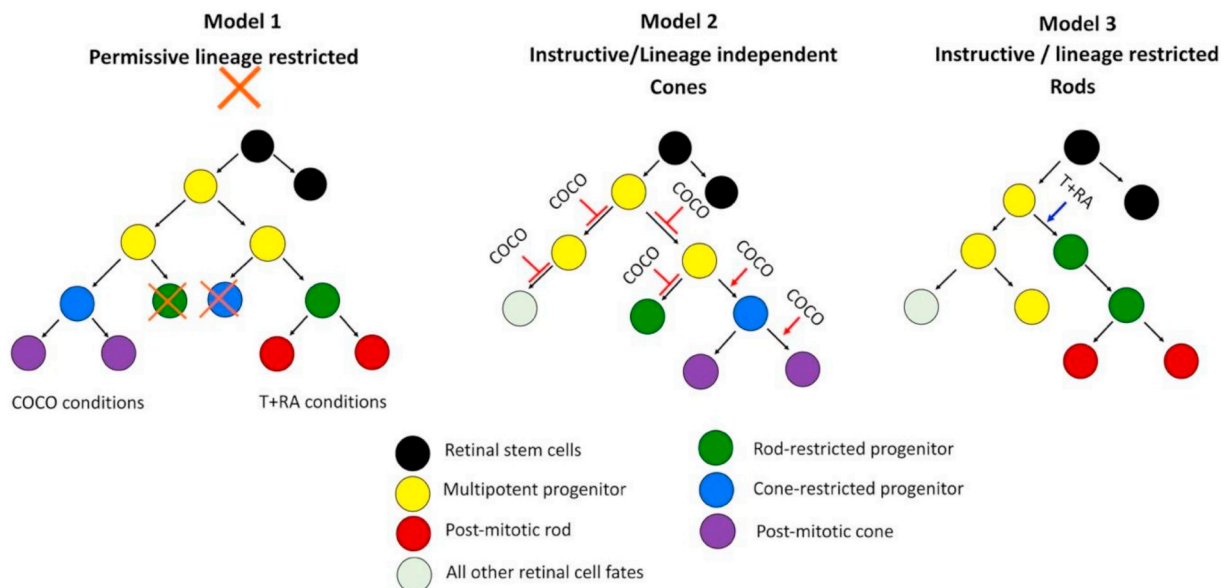
Fig. 7. Alternative models of directed photoreceptor differentiation from RSC progeny. Model 1 represents a permissive mechanism and lineage-restricted mode of differentiation; Model 2 represents an instructive mechanism and lineage-independent mode of differentiation; while Model 3 represents an instructive mechanism and lineage-restricted mode of differentiation. Our results with retroviral clonal analysis and single cell per well analyses support an instructive, rather than a permissive model for rod differentiation. Our data fit Model 3 suggesting an early effect of T + RA in instructing the production of rod-fate-restricted proliferative progenitors, which then divide symmetrically to produce rod-only clones. In the case of cones, our clonal analyses show that there is no difference in survival between non-pigmented progenitors in COCO or pan-retinal conditions, suggesting that COCO does not cause differences in inter- or intra-clonal survival. Moreover, COCO must be continuously present throughout the differentiation period, suggesting that it may act to promote the cone fate of the non-pigmented progenitors through suppression of alternate retinal fates. These findings support an instructive mechanism and lineage-independent mode of differentiation for cone photoreceptors (Model 2).

remaining undifferentiated cell (the stem cell) in this clone and the low frequency of RSCs compared to RPE progenitors might suggest instead that an early RPE progenitor was instructed to produce a large rod-only clone in T + RA.

Our results indicate that exogenous factors can influence retinal progenitor fate restriction and, moreover, that rod and cone lineage-restricted cells may exist during retinal stem cell differentiation in vivo. Moreover, there is a striking similarity between adult RSC-derived photoreceptor differentiation, and photoreceptor differentiation from embryonic neural retinal progenitor cells in vitro, in terms of their differentiation potential (Altshuler et al., 1993; Kelley et al., 1994) and factors governing progenitor proliferation (Wang et al., 2005). The early in vivo birth of cone photoreceptors compared to other retinal cell types might be explained by a default of some retinal progenitors to cone fate before the instructive signals for other retinal lineages are turned on (Akimoto et al., 2006; Mears et al., 2001; Brzezinski and Reh, 2015).

Much of our analyses of cell type composition in varying differentiation conditions utilize immunofluorescence and qPCR-based methods, which limit one to a small number of specific retinal markers. Therefore, we carried out RNA-sequencing to allow for a more robust and complete evaluation of how transcriptionally similar the cones we make from stem cells are to their endogenous counterparts in the mature retina. These data show that, at both the level of individual genes and genetic pathways, the RSC-derived cones are highly correlated with cones isolated from the mature mammalian retina (Figs. 6D, S3). Furthermore, through comparison to the initiating and undifferentiated retinal progenitors, RNA-seq may enable us to identify novel markers involved in cone development and function. It is noteworthy that of the top 20 differentially expressed genes (compared to RSC spheres), 11 are shared between RSC-derived and endogenous cones. While none of these appear known to be involved in cone development or function, the large overlap warrants further investigation. Furthermore, the sequencing data from cones encourages similar analysis on rods derived from RSCs.

5. Conclusion

Overall, these results also contribute to the resolution of conflicting models of cellular determination in the retina, by showing that there may exist numerous pre-programmed (lineage-restricted) progenitors for various retinal lineages. In this study, we demonstrate instructive environmental cues influencing specific fates among retinal progenitors. Our results are consistent with the model developed by (Cepko et al., 1996), as we demonstrate that it is early, rather than late, progenitors in vitro that are able to respond to environmental cues to undergo lineage restriction to rod-specific retinal progenitors (Cepko et al., 1996). Taken together, analyses of RSC and neural retinal progenitor differentiation represent a tractable system for studying the response of rod and cone-restricted progenitors to environmental cues at the clonal level, and the molecular mechanisms by which uncommitted progenitors make the decisions between proliferation, survival, and fate selection.

Competing interests

There are no financial or non-financial competing interests for all authors of this manuscript.

Appendix A. Supplementary data

Supplementary data to this article can be found online at https://doi.org/10.1016/j.scr.2018.11.005.

References

Abdouh, M., Bernier, G., 2006. In vivo reactivation of a quiescent cell population located in the ocular ciliary body of adult mammals. Exp. Eye Res. 83, 153–164.

Ahmad, I., Tang, L., Pham, H., 2000. Identification of neural progenitors in the adult mammalian eye. Biochem. Biophys. Res. Commun. 270, 517–521.

Akimoto, M., Cheng, H., Zhu, D.X., Brzezinski, J.A., Khanna, R., Filippova, E., Oh, E.C.T., Jing, Y.Z., Linares, J.L., Brooks, M., Zareparsi, S., Mears, A.J., Hero, A., Glaser, T., Swaroop, A., 2006. Targeting of GFP to newborn rods by Nrl promoter and temporal expression profiling of flow-sorted photoreceptors. Proc. Natl. Acad. Sci. U. S. A. (103), 3890–3895.

Altshuler, D., Loturco, J.J., Rush, J., Cepko, C., 1993. Taurine Promotes the Differentiation of a Vertebrate Retinal Cell-Type in-Vitro, Development. 119. pp. 1317–1328.

Ballios, B.G., Clarke, L., Coles, B.L., Shoichet, M.S., Van Der Kooy, D., 2012. The adult retinal stem cell is a rare cell in the ciliary epithelium whose progeny can differentiate into photoreceptors. Biol. Open 1, 237–246.

Ballios, B.G., Cooke, M.J., Donaldson, L., Coles, B.L.K., Morshead, C.M., van der Kooy, D., Shoichet, M.S., 2015. A hyaluronan-based injectable hydrogel improves the survival and integration of stem cell progeny following transplantation. Stem Cell Rep. 4, 1031–1045.

Bassett, E.A., Wallace, V.A., 2012. Cell fate determination in the vertebrate retina. Trends Neurosci. 35, 565–573.

Bazhulina, N.P., Nikitin, A.M., Rodin, S.A., Surovaya, A.N., Kravatsky, Y.V., Pismensky, V.F., Archipova, V.S., Martin, R., Gursky, G.V., 2009. Binding of Hoechst 33258 and its derivatives to DNA. J. Biomol. Struct. Dyn. 26, 701–718.

Brzezinski, J.A., Reh, T.A., 2015. Photoreceptor cell fate specification in vertebrates. Development 142, 3263–3273.

Cepko, C.L., Austin, C.P., Yang, X.J., Alexiades, M., 1996. Cell fate determination in the vertebrate retina. Proc. Natl. Acad. Sci. U. S. A. 93, 589–595.

Cicero, S.A., Johnson, D., Reyntjens, S., Frase, S., Connell, S., Chow, L.M.L., Baker, S.J., Sorrentino, B.P., Dyer, M.A., 2009. Cells previously identified as retinal stem cells are pigmented ciliary epithelial cells. Proc. Natl. Acad. Sci. U. S. A. 106, 6685–6690.

Cohen, A.R., Gomes, F.L., Roysam, B., Cayouette, M., 2010. Computational prediction of neural progenitor cell fates. Nat. Methods 7, 213–218.

Coles, B.L., Angenieux, B., Inoue, T., Del Rio-Tsonis, K., Spence, J.R., McInnes, R.R., Arsenijevic, Y., van der Kooy, D., 2004. Facile isolation and the characterization of human retinal stem cells. Proc. Natl. Acad. Sci. U. S. A. 101, 15772–15777.

Coles, B.L.K., Horsford, D.J., McInnes, R.R., van der Kooy, D., 2006. Loss of retinal progenitor cells leads to an increase in the retinal stem cell population in vivo. Eur. J. Neurosci. 23, 75–82.

Del Debbio, C.B., Peng, X., Xiong, H.G., Ahmad, I., 2013. Adult ciliary epithelial stem cells generate functional neurons and differentiate into both early and late born retinal neurons under non-cell autonomous influences. BMC Neurosci. 14.

Demontis, G.C., Aruta, C., Comitato, A., De Marzo, A., Marigo, V., 2012. Functional and molecular characterization of rod-like cells from retinal stem cells derived from the adult ciliary epithelium. PLoS ONE 7, e33338.

Fang, Y., Cho, K.S., Tchedre, K., Lee, S.W., Guo, C., Kinouchi, H., Fried, S., Sun, X., Chen, D.F., 2013. Ephrin-A3 suppresses Wnt signaling to control retinal stem cell potency. Stem Cells 31, 349–359.

Gomes, F.L., Zhang, G., Carbonell, F., Correa, J.A., Harris, W.A., Simons, B.D., Cayouette, M., 2011. Reconstruction of rat retinal progenitor cell lineages in vitro reveals a surprising degree of stochasticity in cell fate decisions. Development 138, 227–235.

Gualdoni, S., Baron, M., Lakowski, J., Decembrini, S., Smith, A.J., Pearson, R.A., Ali, R.R., Sowden, J.C., 2010. Adult ciliary epithelial cells, previously identified as retinal stem cells with potential for retinal repair, fail to differentiate into new rod photoreceptors. Stem Cells 28, 1048–1059.

Hänzelmann, S., Castelo, R., Guinney, J., 2013. GSVA: gene set variation analysis for microarray and RNA-seq data. BMC Bioinforma. 14, 7. https://doi.org/10.1186/1471-2105-14-7. http://www.biomedcentral.com/1471-2105/14/7.

Holowacz, T., Huelsken, J., Dufort, D., van der Kooy, D., 2011. Neural stem cells are increased after loss of beta-catenin, but neural progenitors undergo cell death. Eur. J. Neurosci. 33, 1366–1375.

Holt, C.E., Bertsch, T.W., Ellis, H.M., Harris, W.A., 1988. Cellular determination in the Xenopus retina is independent of lineage and birth date. Neuron 1, 15–26.

Inoue, T., Coles, B.L., Dorval, K., Bremner, R., Bessho, Y., Kageyama, R., Hino, S., Matsuoka, M., Craft, C.M., McInnes, R.R., Tremblay, F., Prusky, G.T., van der Kooy, D., 2010. Maximizing functional photoreceptor differentiation from adult human retinal stem cells. Stem Cells 28, 489–500.

Kelley, M.W., Turner, J.K., Reh, T.A., 1994. Retinoic Acid Promotes Differentiation of Photoreceptors in-Vitro, Development. 120. pp. 2091–2102.

Kim, J.W., Yang, H.J., Oel, A.P., Brooks, M.J., Jia, L., Plachetzki, D.C., Li, W., Allison, W.T., Swaroop, A., 2016. Recruitment of rod photoreceptors from short-wavelength-sensitive cones during the evolution of nocturnal vision in mammals. Dev. Cell 37, 520–532.

McUsic, A.C., Lamba, D.A., Reh, T.A., 2012. Guiding the morphogenesis of dissociated newborn mouse retinal cells and hES cell-derived retinal cells by soft lithography-patterned microchannel PLGA scaffolds. Biomaterials 33, 1396–1405.

Mears, A.J., Kondo, M., Swain, P.K., Takada, Y., Bush, R.A., Saunders, T.L., Sieving, P.A., Swaroop, A., 2001. Nrl is required for rod photoreceptor development. Nat. Genet. 29, 447–452.

Merico, D., Isserlin, R., Stueker, O., Emili, A., Bader, G.D., 2010. Enrichment map: a network-based method for gene-set enrichment visualization and interpretation. PLoS One 5 (11), e13984 (2010 Nov 15).

Mo, A., Luo, C., Davis, F.P., Mukamel, E.A., Henry, G.L., Nery, J.R., Urich, M.A., Picard, S., Lister, R., Eddy, S.R., Beer, M.A., Ecker, J.R., Nathans, J., 2016. Epigenomic landscapes of retinal rods and cones. elife 5, e11613.

Opas, M., Dziak, E., 1994. Bfgf-induced transdifferentiation of Rpe to neuronal progenitors is regulated by the mechanical-properties of the substratum. Dev. Biol. 161, 440–454.

Park, C.M., Hollenberg, M.J., 1989. Basic fibroblast growth factor induces retinal regeneration in vivo. Dev. Biol. 134, 201–205.

Smiley, S., Nickerson, P.E., Comanita, L., Daftarian, N., El-Sehemy, A., Tsai, E.L., Matan-Lithwick, S., Yan, K., Thurig, S., Touahri, Y., Dixit, R., Aavani, T., De Repentingy, Y., Baker, A., Tsilfidis, C., Biernaskie, J., Sauve, Y., Schuurmans, C., Kothary, R., Mears, A.J., Wallace, V.A., 2016a. Establishment of a cone photoreceptor transplantation platform based on a novel cone-GFP reporter mouse line. Sci. Rep. 6, 22867.

Smiley, S., Nickerson, P.E., Comanita, L., Daftarian, N., El-Sehemy, A., Tsai, E.L., Matan-Lithwick, S., Yan, K., Thurig, S., Touahri, Y., Dixit, R., Aavani, T., De Repentigny, Y., Baker, A., Tsilfidis, C., Biernaskie, J., Sauve, Y., Schuurmans, C., Kothary, R., Mears, A.J., Wallace, V.A., 2016b. Corrigendum: establishment of a cone photoreceptor transplantation platform based on a novel cone-GFP reporter mouse line. Sci. Rep. 6, 24012.

Sparrow, J.R., Hicks, D., Barnstable, C.J., 1990. Cell commitment and differentiation in explants of embryonic rat neural retina. Comparison with the developmental potential of dissociated retina. Brain Res. Dev. Brain Res. 51, 69–84.

Swaroop, A., Kim, D., Forrest, D., 2010. Transcriptional regulation of photoreceptor development and homeostasis in the mammalian retina. Nat. Rev. Neurosci. 11, 563–576.

Szel, A., Vanveen, T., Rohlich, P., 1994. Retinal cone differentiation. Nature 370 (336–336).

Szel, A., Lukats, A., Fekete, T., Szepessy, Z., Rohlich, P., 2000. Photoreceptor distribution in the retinas of subprimate mammals. J. Opt. Soc. Am. A Opt. Image Sci. Vis. 17, 568–579.

Tropepe, V., Coles, B.L., Chiasson, B.J., Horsford, D.J., Elia, A.J., McInnes, R.R., van der Kooy, D., 2000. Retinal stem cells in the adult mammalian eye. Science 287, 2032–2036.

Turner, D.L., Cepko, C.L., 1987. A common progenitor for neurons and glia persists in rat retina late in development. Nature 328, 131–136.

Turner, D.L., Snyder, E.Y., Cepko, C.L., 1990. Lineage-independent determination of cell type in the embryonic mouse retina. Neuron 4, 833–845.

Wall, D.S., Mears, A.J., McNeill, B., Mazerolle, C., Thurig, S., Wang, Y.P., Kageyama, R., Wallace, V.A., 2009. Progenitor cell proliferation in the retina is dependent on Notch-independent Sonic hedgehog/Hes1 activity. J. Cell Biol. 184, 101–112.

Wang, Y.P., Dakubo, G.D., Thurig, S., Mazerolle, C.J., Wallace, V.A., 2005. Retinal ganglion cell-derived sonic hedgehog locally controls proliferation and the timing of RGC development in the embryonic mouse retina. Development 132, 5103–5113.

Wetts, R., Fraser, S.E., 1988. Multipotent precursors can give rise to all major cell types of the frog retina. Science 239, 1142–1145.

Zhou, S., Flamier, A., Abdouh, M., Tetreault, N., Barabino, A., Wadhwa, S., Bernier, G., 2015. Differentiation of human embryonic stem cells into cone photoreceptors through simultaneous inhibition of BMP, TGFbeta and Wnt signaling. Development 142, 3294–3306.